Chapter

Physical Processes and Plasma Parameters in a Radio-Frequency Hybrid Plasma System for Thin-Film Production with Ion Assistance

Elena Kralkina, Andrey Alexandrov, Polina Nekludova, Aleksandr Nikonov, Vladimir Pavlov, Konstantin Vavilin, Vadim Odinokov and Vadim Sologub

Abstract

The results of the study of the plasma reactor on the combined magnetron discharge and radio-frequency (RF) inductive discharge located in the external magnetic field are presented. Magnetron discharge provides the generation of atoms and ions of the target materials, while the flow of accelerated ions used for the ion assistance is provided by the RF inductive discharge located in an external magnetic field. Approaching the region of resonant absorption of RF power by optimizing the magnitude and configuration of the external magnetic field makes it possible to obtain a uniform within 10% radial distribution of the ion current across the diameter of 150 mm. When the RF power supply power is 1000 W, the ion current density on the substrate can be adjusted in the range of 0.1–3 mA/cm^2. The use of ion assisting results in a fundamental change in the structure and properties of functional coatings, deposited using a magnetron.

Keywords: RF inductive discharge, assisting ions, helicon, Trivelpiece-Gould wave, magnetic field, magnetron, film deposition

1. Introduction

At the present time, vacuum plasma methods for the formation of multicomponent thin-film structures based on magnetron or vacuum arc gas discharges are widely used in the industry. These methods allow to obtain a wide class of functional coatings, such as optical, hardening, anticorrosion, antibacterial, etc. A particular case of the known vacuum plasma methods of coating formation is ion-assisted deposition [1–8]. The method involves continuous or periodic bombardment of growing thin films by accelerated ions.

The results of the bombardment of the substrate and the growing films by accelerated ions are [1–8]:

- cleaning of the substrate surface and removing traces of water and hydrocarbons;
- increase of density and, in some cases, modification of the growing film structure;
- removal of loosely bounded molecules during the film growth;
- improving the adhesion of the film to the substrate;
- better control of the film stoichiometric composition in the case of chemically active gas usage.

The concept of ion-stimulated deposition was proposed more than 70 years ago by Berghaus [1]. More than two decades later, the technology was implemented in the experimental works by Mattox and MacDonald [2], as well as by Mattox and Kominiak [3].

Currently, vacuum deposition of films is carried out by way of thermal evaporation, magnetron, vacuum arc, and ion-beam deposition [4–8]. Bombardment of substrates and growing films is implemented using accelerated ion beams, generated in ion sources or gas-discharge plasma. In the latter case, a negative bias is applied to the substrate, which accelerates the ions in the direction perpendicular to the surface of the growing film.

The effect of the ion flux treatment on the thin-film properties substantially depends on the flux magnitude, energy and mass of the ions, as well as the ratio between the flows of the assisting ions and the atoms of the deposited substance. The question of the optimal magnitude of energy, which has to be introduced into the growing film per a single deposited atom, was examined in [5, 9–12].

In [10], the results of numerous experiments on the deposition of coatings using ion beam stimulation are analyzed. It is shown that the most significant changes in the properties of deposited films occur, when each of the deposited atom obtains additional energy in the range of 1.0–100 eV. However, it was shown in [11] that in the case of Ti-Al-N film deposition, composition of the film, predominant orientation, and distances between atoms in the lattice significantly depend on whether the energy is introduced by one high-energy ion or by several low-energy ions. As shown in [12], the problem is that in the above cases the energy is transferred to the deposited atoms irregularly. High-energy ions are capable of creating defects in the deeper layers of the coating and the substrate; having been reflected from the surface of the substrate, the ions acquire energy, which significantly depends on the substrate material. This results in the fact [12] that the energy required for the film growth at the initial stage may greatly differ from the energy, which is required at the final growth stage, when the assisting ions interact only with the atoms of the deposited substance. It should be noted that when the ion energy exceeds 15–30 eV [13], the growing film can be sputtered with a beam of fast ions. The use of ion beams with energies up to 30 eV makes it possible to reduce these effects to a minimum.

The use of vacuum plasma methods of forming functional coatings in the industry requires the ensuring of high-speed film deposition and, accordingly, the use of significant fluxes of assisting ions. Literature review [6, 13] shows that the ion fluxes generated by gridded and gridless ion beam sources are often insufficient to assist the growth of films produced using magnetron and vacuum arc methods. Besides, there is a complex problem of matching the operation of gas-discharge sources generating assisting ions and coating systems in terms of pressure.

In [14], the possibility of generating plasma flows with the ion component density of up to 20–30 mA/cm^2 and independently controlled ion energy within the range of 20–120 eV by using a combination of arc discharge with inductive radio-frequency (RF) discharge in external magnetic field is shown. The results obtained in [14] served as the starting point for the development of a plasma reactor [15–18], intended for the magnetron sputtering of functional coatings using stimulation by ions, generated in RF inductive discharge with external magnetic field.

2. Basic physical patterns underlying the design of a plasma reactor

The task of developing a plasma reactor for magnetron sputtering deposition of ion-stimulated coatings has determined the composition of the reactor: one or more magnetron sources to provide the flow of sputtered particles onto a substrate and gas-discharge source, which provides the generation of a magnitude-controlled flux of ions, bombarding the substrate. The ion flux energy control is provided by a direct current (DC) or RF biasing of the substrate.

To enable successful operation of the plasma reactor, it is necessary to ensure that:

1. The working areas of the magnetron and gas-discharge sources are matched in terms of pressure.

2. Changing of external parameters of the gas-discharge source ensures coordination of the flux of assisting ions and the flux of sputtered particles entering the substrate.

3. Changing of external parameters of the gas-discharge source ensures uniform density of ion current density on the substrate not worse than 10%.

4. The plasma reactor operates using both inert and chemically active gases.

Let us do some estimates. Taking into account typical rate of magnetron sputtering, it is advisable to ensure that the density of the stimulating ion current varies within the range of 0.1–3 mA/cm^2. This means that the plasma density must vary within the range of $0.03–1 \times 10^{11}$ cm^{-3}.

A literature review [19–21] has shown that it is reasonable to consider two modifications of inductive RF discharge as the options for implementing the working process in the gas-discharge source, namely, inductive RF discharge in the absence and in the presence of external magnetic field. In the first case, the magnitude of the assisting ion flow will be determined by the power of the RF power supply. In the second case, two external parameters—the power of the RF power supply and the induction of an external magnetic field—will allow to control the values of plasma parameters and their spatial distribution in the plasma reactor.

In modern industrial installations, the diameter of substrates usually exceeds 200 mm. Large diameter of the plasma reactor makes it difficult to generate strong magnetic fields in the volume of the reactor. It is known [22–25] that when an external magnetic field with induction of less than 100 Gs is imposed on inductive RF discharge, a peak of electron density is observed at certain resonant values of the magnetic field. The absolute values of plasma density are close to those required in case of our task. The physically observable density peak is associated with resonant excitation in the plasma reactor of helicon and Trivelpiece-Gould waves [22–25]. Provided that the pressure in the reactor does not exceed 10 mTorr, the

Trivelpiece-Gould wave is a bulk wave, penetrates deep into plasma, and determines the absorption of RF power [24, 25].

In [26], the authors offered a scheme of two-chamber process plasma source, based on inductive RF discharge with external magnetic field, diverging toward the substrate. Following the scheme [26], preliminary experiments on the study of the discharge parameters have been carried out with the plasma reactor having two chambers [27]. The model consisted of two cylindrical quartz chambers of different diameters and a magnetic system. The upper part of the reactor (gas-discharge chamber) had a diameter of 10 cm and a height of 25 cm. The lower part of the reactor (process chamber) had 46 cm diameter and 30 cm height. The RF power input unit—a three-turn solenoid antenna—was located on the outer surface of the gas-discharge chamber. The magnetic system allowed generation in the volume of the process chamber of uniform magnetic field, converging and diverging toward the lower flange where the substrate was located.

Experiments have shown that when using an inductive RF discharge in the absence of magnetic field, the discharge is concentrated in the gas-discharge chamber, while the plasma density in the process chamber near the substrate is vanishingly small. A different situation is observed when using external magnetic field, diverging in the region of the gas-discharge chamber and uniform in the region of the process chamber. Under argon pressures, when the electron mean free path exceeds the longitudinal size of the system, the imposition of magnetic field results in significant changes in the discharge length [27]. In the absence of magnetic field, the discharge is concentrated in the gas-discharge chamber. An increase in the magnitude of the magnetic field first results in the appearance of plasma in the upper part of the technological chamber. Then, the length of the intensely glowing part of the discharge in the process chamber starts to grow, and, finally, the discharge closes at the bottom flange. The movement of electrons across the magnetic field is difficult; therefore, an extended plasma column, sharply outlined in the radial direction, appears in the process chamber. In parallel

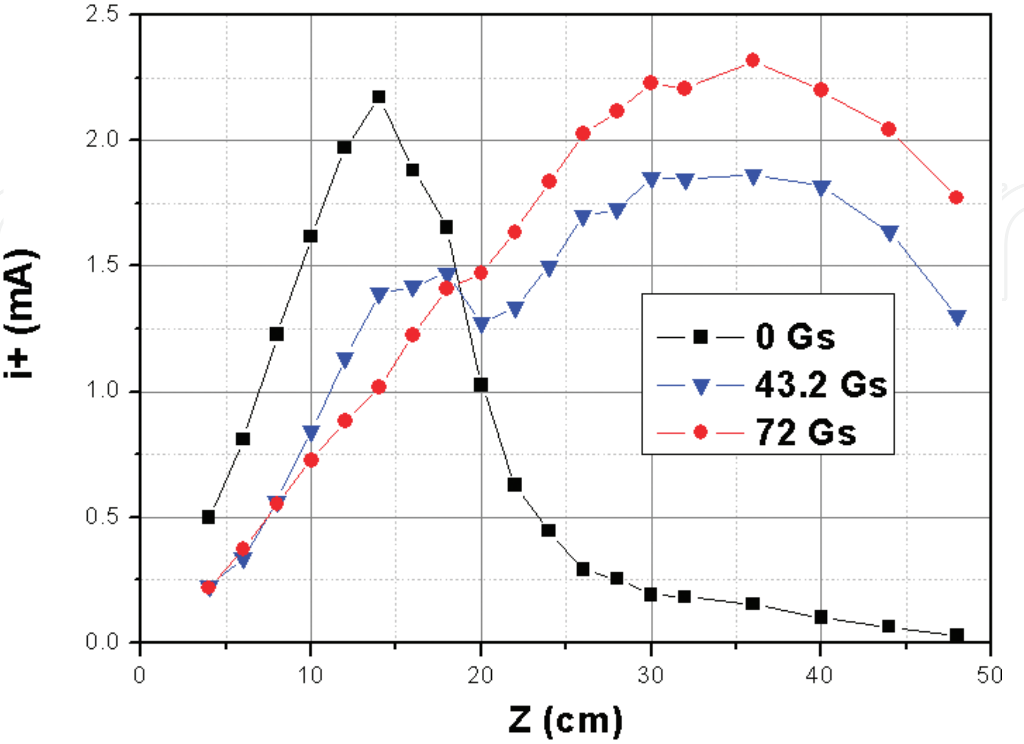

Figure 1.
Probe ionic saturation current distribution along z axis of plasma source depending on external magnetic field magnitude: 0.7 mTorr, 400 W, and 13.56 MHz.

with the increase in the discharge length near the substrate, an increase in the probe ion saturation current is observed.

Figure 1 shows variation of the axial distribution of the probe ion saturation current when the magnetic field induction grows. In the absence of magnetic field, the discharge is concentrated in the upper part of the plasma source; as the magnetic field increases, the ion current in the lower chamber gets increased. When the magnetic field exceeds 36 Gs, the discharge gets localized in the process chamber of the reactor.

This effect is observed for all of the examined powers of the RF power supply, and the maximum values of the ion current are increasing in proportion to the input power. The achieved plasma concentrations near the substrate correspond to those required in this work. Detailed studies of the physical causes for the axial redistribution of plasma density as the magnetic field induction increases have shown that the effect is associated with the patterns of excitation of partial standing waves in the plasma [17, 27]. It should be noted that the use of other configurations of the magnetic field did not result in significant increase in the ionic saturation current near the substrate.

The obtained results served as the basis for the development of a semi-industrial installation for magnetron deposition of coatings with ion assistance.

3. Design of a plasma reactor, which combines magnetron and inductive RF discharge with external magnetic field

Preliminary results, obtained using a plasma reactor prototype, have served as the basis for a semi-industrial installation [16–18]. Diagram of this prototype is shown in **Figure 2**. The reactor consists of two parts. The main part is a metal cylindrical process chamber having 500 mm diameter and 350 mm height. At the bottom of the chamber, there is a rotating table for the accommodation of samples being treated. To facilitate spectrometric studies of plasma parameters, two optical inspection windows are located above the table right opposite to each other. The magnetron source is installed on the side surface of the process chamber.

Quartz gas-discharge chamber having 250 mm length and 220 mm diameter is mounted on top of the process chamber. From above the chamber, volume is covered with a glass blind flange; from beneath the chamber is sealed with a metal flange with an opening that allows plasma to penetrate into the main chamber.

Below the process chamber, a pumping system is installed, consisting of rotary and turbo molecular pumps. The working gas is supplied to the reactor through the gas inlet located in the upper part of the gas-discharge chamber.

The magnetic system consists of two electromagnets, located in the upper and lower parts of the process chamber. The electromagnets ensure generation of diverging magnetic field in the area of the gas-discharge chamber. The magnitude of the magnetic field in each specific point in the volume of the process chamber is determined by the currents I_{top}, I_{bot} flowing through the top and bottom electromagnets, respectively, and one and the same value of magnetic induction can be provided by setting different ratios between the currents of the magnets. In this regard, in the further section, the dependence of the discharge parameters on I_{top}, I_{bot} is given in the graphs illustrating the results of experiments. **Table 1** contains the magnetic field induction values achieved near the antenna, in the center of the process chamber and near the substrate at different values of I_{top}, I_{bot}.

To excite an inductive RF discharge, a solenoid antenna is used, which is located on the outer surface of the quartz chamber. The ends of the antenna are connected

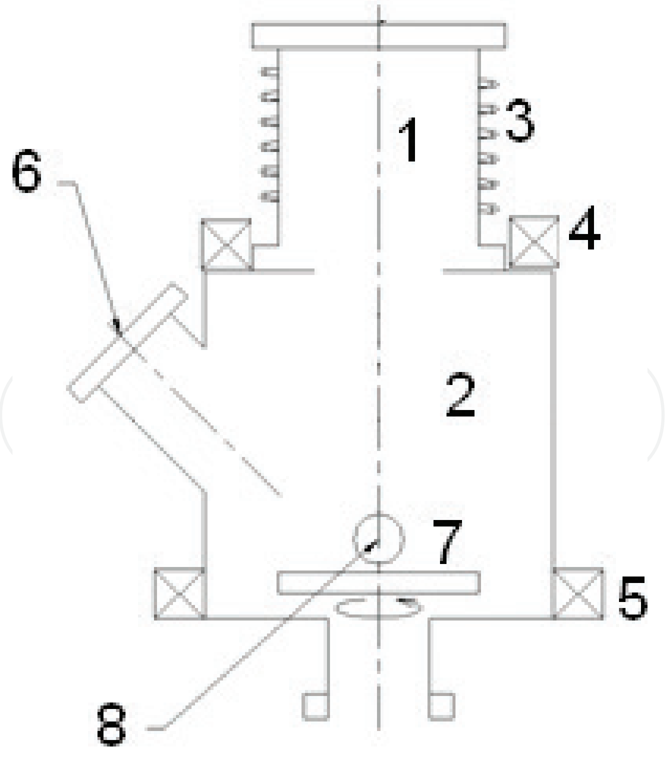

Figure 2.
Plasma reactor prototype diagram: (1, 2) gas-discharge and process chambers, (3) antenna, (4, 5) top and bottom electromagnets, (6) magnetron, (7) rotating table, and (8) window.

Top magnet current (Gs)	Bottom magnet current (Gs)	Magnetic field in the substrate plane (Gs)	Magnetic field in the bottom part of the gas-discharge chamber (Gs)
3	5	39	49
4	5	40	63
5	5	42	78
7	5	45	107
3	1	11	45
3	3	25	47
3	7	53	50
3	9	66	52
3	12	87	55
10	4	42	150
1	6	42	20

Table 1.
Correlation between the currents of the magnets and the magnitude of the magnetic field near the substrate and in the gas-discharge chamber.

through the matching system to the RF power source, having the operating frequency of 13.56 MHz and an output power of up to 1000 W. In the inductive RF discharge, the power of RF power sources is coupled not only to plasma but is wasted in the antenna too. In order to measure the RF power value P_{pl} coupled to plasma, the method described in [24] was used.

To ignite and maintain the magnetron discharge, the RF power source with the operating frequency of 13.56 MHz and output power up to 1000 W is used.

To study the homogeneity of plasma near the substrate, a movable Langmuir probe was used, capable of traveling along the diameter of the substrate. When measuring the dependence of the probe ionic saturation current on the magnitude and configuration of the magnetic field, 60 V potential negative in respect of to the walls of the main chamber is applied to the probe.

In parallel with probe measurements, the plasma glow spectrum was studied. Plasma radiation via an optical fiber was fed to the input of the MDR-40 monochromator, on the output of which photomultiplier FEU-100 was installed. The signal from the photomultiplier was amplified and fed to an ADC connected to a computer. The spectrum was scanned in the wavelength range of 400–700 nm. In addition to the glow spectrum, longitudinal distribution of the spectral lines intensity was measured. To this end, the light guide was moved along the generating line of the process chamber within the diagnostic window opening.

Thin films were deposited onto silicon substrates when only the magnetron was operating and when the magnetron and the gas-discharge plasma source were operating together in the absence and in the presence of bias on the substrate. The morphology of the surface and the cleavage of the films were studied with the help of scanning electron microscope Supra-40. The electro-physical characteristics of the coatings were measured with the help of a two-probe method.

4. Results of the gas-discharge plasma source studies.

At the first stage of the study, the parameters of the plasma generated by inductive RF discharge were studied depending on the size and configuration of the external magnetic field, the power of the RF power supply, and the pressure of argon in the absence of the magnetron discharge.

Experimental studies of the discharge have shown that when a longitudinal magnetic field is imposed on the discharge, an extended plasma column is formed in the process chamber, similar to that observed in the prototype reactor. The diameter of the plasma column is approximately equal to the diameter of the quartz chamber that is 20 cm (**Figure 3**).

As with the prototype, a change in the magnetic field made it possible to control the longitudinal distribution of plasma density. **Figure 4** shows correlation between the plasma glow intensity I_1, measured in the central part of the process chamber, and at the substrate I_3. An increase in the currents through the magnet, located near the gas discharge I_{top} and the substrate I_{bot}, results in equalization of the distribution of the plasma glow intensity along the discharge axis. This confirms the conclusion about the formation of the plasma "column," closing on the substrate.

Figures 5 and **6** show the dependence of the portion of the power P_{pl} coupled to the argon plasma, on the values of the currents I_{top}, I_{bot} through the top and bottom magnets, provided that the power of the RF power supply is 1000 W. As can be seen, P_{pl} is determined by the magnetic field B, which is generated by the current through the top electromagnet located in the area of the gas-discharge chamber. The effect induced by the bottom magnet is noticeable at low currents of the top magnet, when contribution of the bottom electromagnet to the values of the magnetic field induction is significant. The non-monotonic character of dependence of the absorbed power on B is also worth noticing. P_{pl} reaches the maximum in the I_{top} range between 3 and 5 A, which corresponds to magnetic fields in the area of the gas-discharge chamber of 50–80 Gs. The non-monotonous nature of the dependence of the absorbed power on the external magnetic field is retained when argon is replaced by other working gases, such as neon, argon, and oxygen. However, the position of the energy input maximum significantly depends on the working

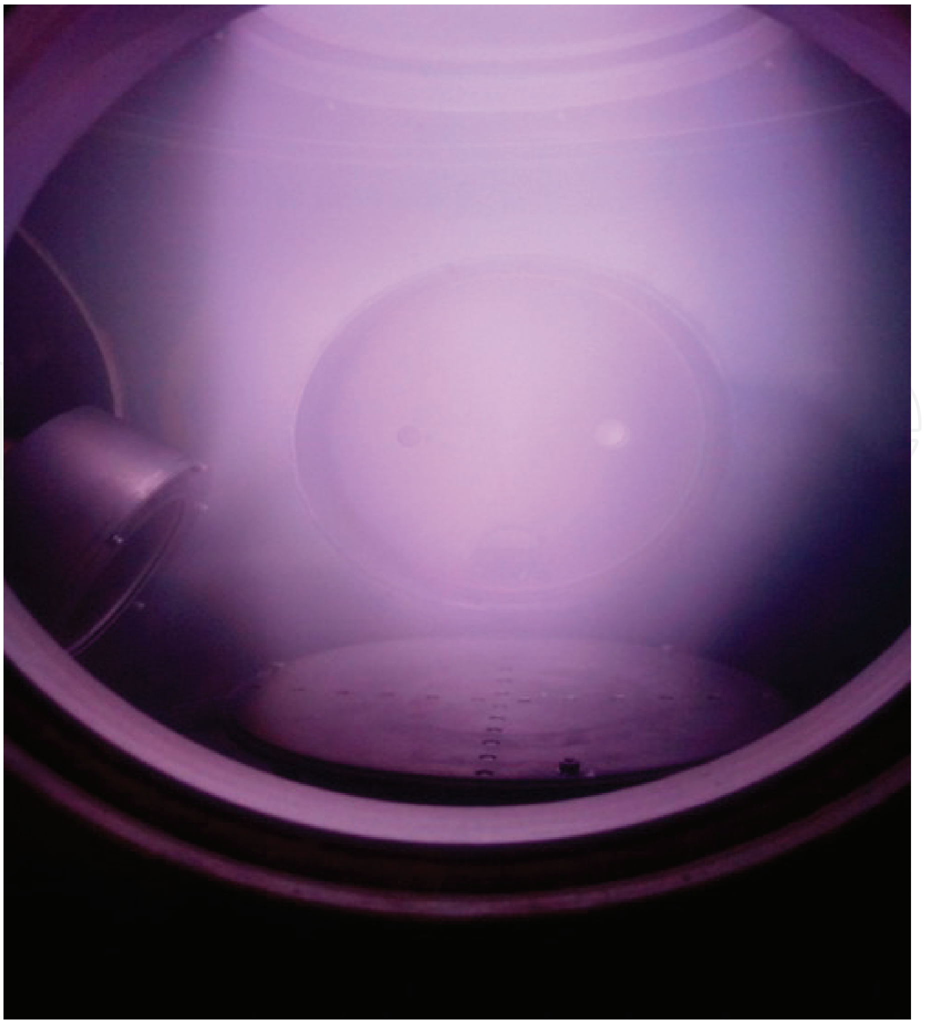

Figure 3.
Photo of the discharge in the plasma reactor.

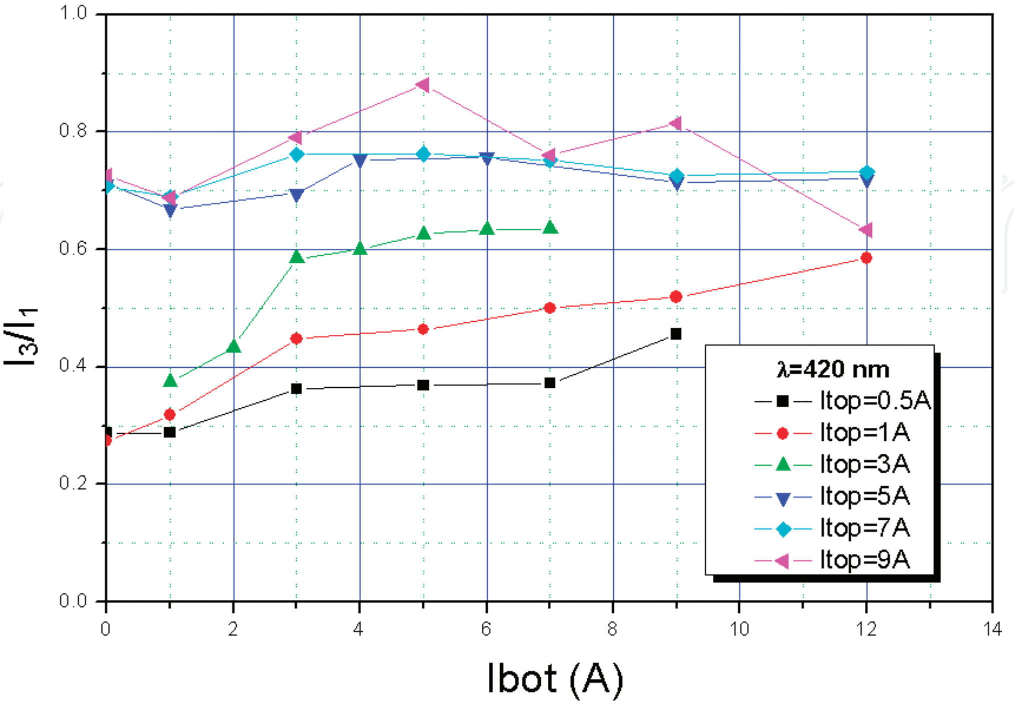

Figure 4.
The ratio of plasma glow intensity near the substrate I_3 to the plasma glow intensity near the magnetron I_1 versus the current flowing through the bottom electromagnet. Corresponding values of the current through the top electromagnet are shown in the menu in the figure. Pressure, 0.2 Pa.

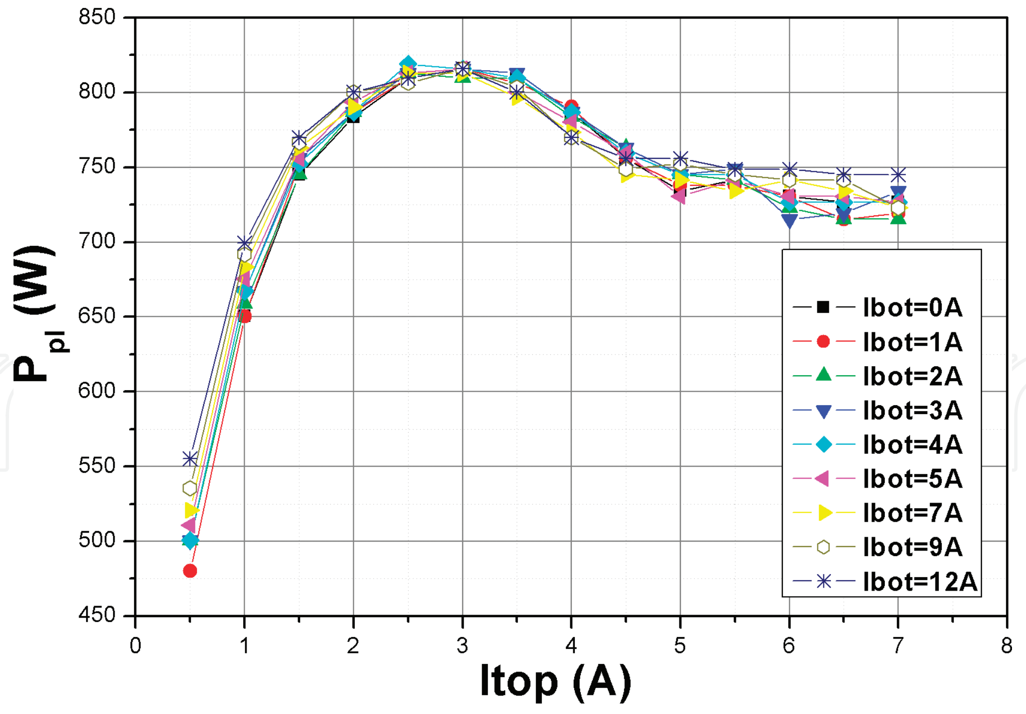

Figure 5.
Dependence of the portion of power, coupled to plasma, on the values of currents through the top and bottom magnets, provided that the RF power supply power is 1000 W. Argon pressure, 0.7 Pa.

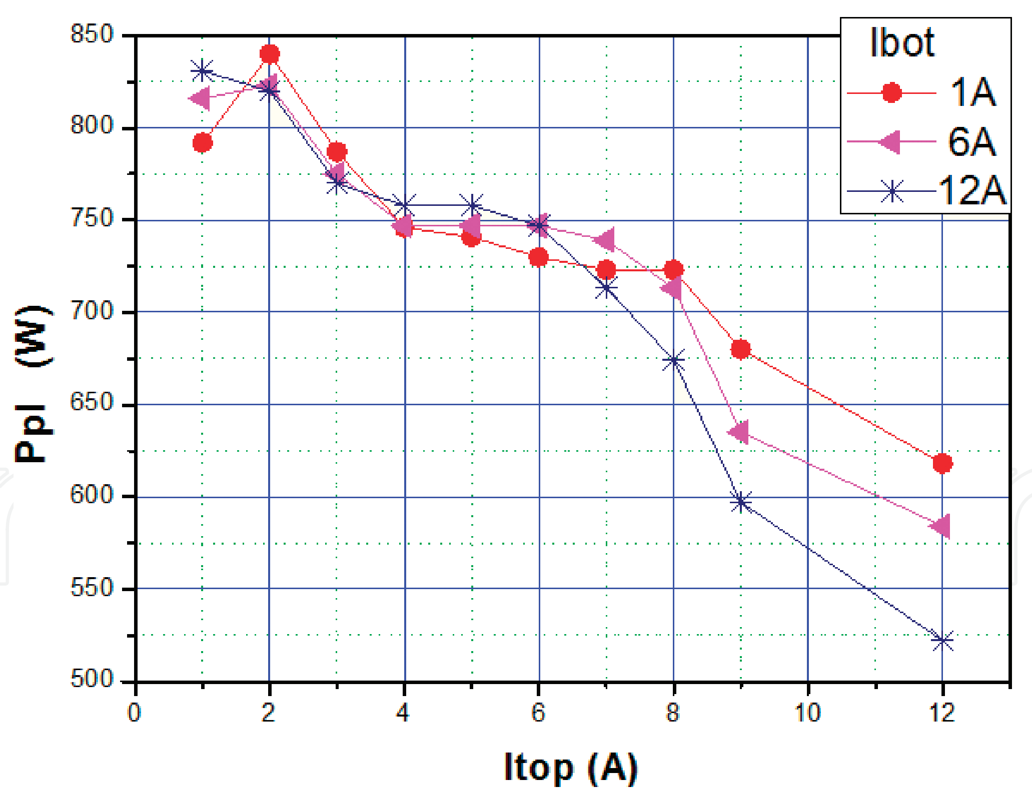

Figure 6.
Dependence of the portion of power, coupled to plasma, on the values of currents through the top and bottom magnets, provided that the RF power supply power is 1000 W. Oxygen pressure, 0.7 Pa.

gas used. Thus, with the use of oxygen, position of the $P_{pl}(B)$ maximum at the RF power supply power of 1000 W is reached at I_{top} = 2 A (see **Figure 6**).

Figure 7 shows radial dependence of the RF longitudinal magnetic field B_z, measured at various I_{top} values. One can see that B_z under condition of the best absorption of the RF power (at the magnetic field of about 80 G in the area of the

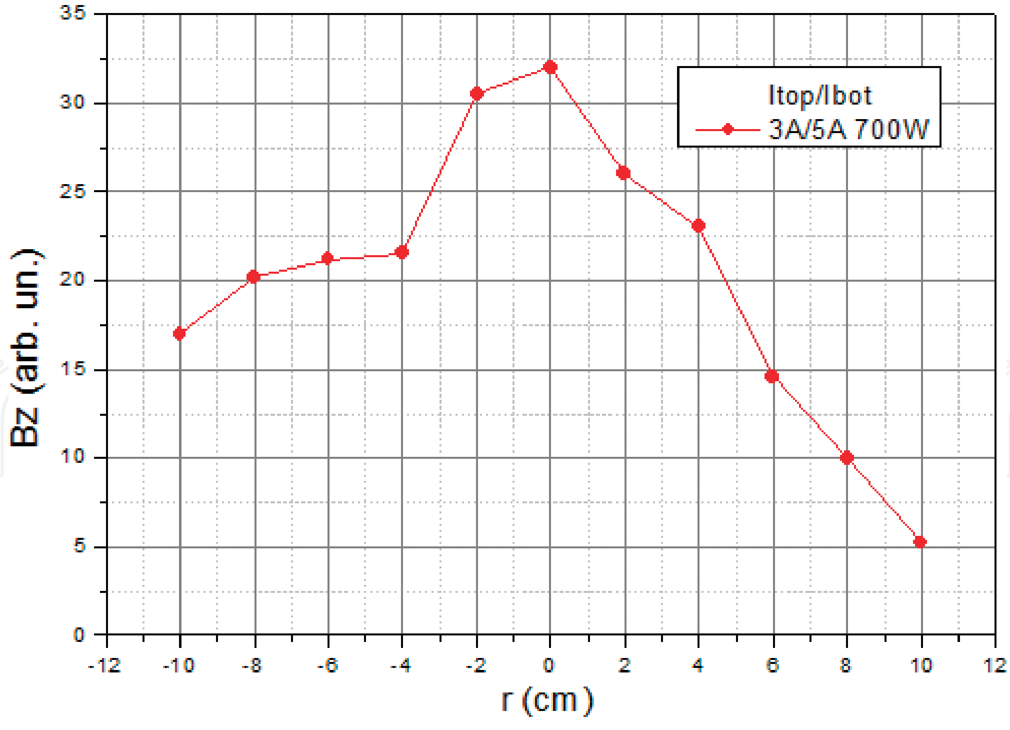

Figure 7.
Radial dependence of the RF longitudinal magnetic field.

gas-discharge chamber) reaches its maximum on the discharge axis, that is, the RF fields penetrate deep into the plasma (see **Figure 7**). This indicates excitation of bulk waves in the discharge.

Calculation of the dependence of the RF fields, excited in plasma, on the external magnetic field, made on the basis of the theoretical model of a limited inductive plasma source with external magnetic field [25], has shown that interconnected helicons and Trivelpiece-Gould waves are excited in the discharge under considered experimental conditions. The Trivelpiece-Gould wave is a bulk wave, and it is the dissipation of its energy that determines the absorption of RF power in the plasma.

The conclusion concerning the resonant excitation of bulk waves at the current of the top magnet of 5A is also confirmed by measurements of the probe ionic saturation current near the substrate (see **Figure 8**). An increase in the current of the top magnet within the range from 1 to 5 A results in increase in the absolute values of the ionic current and the formation of a bell-shaped distribution. As the current is further increased to 7 A, the portion of RF power absorbed by the plasma and the absolute value of the probe ionic saturation current decrease. It is necessary to note the result that is important for technological applications: at the top magnet current of 3A, the most uniform distribution of the ion current is observed. Deviation of the ionic current values from the average ones within the 20 cm diameter does not exceed 10%. Remarkably, the most uniform radial distribution near the substrate is observed not in the resonance region, but when approaching the resonance region.

The most uniform distribution, obtained at the top magnet current of 3A, corresponds to the ionic current density of about 1 mA/cm^2. This value may be insufficient for ionic assistance at high rates of film deposition. Additional experiments have shown that increasing the bottom magnet current allows to increase the ionic current density by two to three times and to obtain homogeneous plasma within the diameter of 15 cm (**Figure 9**, curves 1 and 2).

Figure 9 additionally shows the radial distributions of the ionic saturation current, obtained at the top magnet current of 1A. As a reminder, the point I_{top} = 1 A is located before the maximum of the $P_{pl}(I_{top})$ curve. It is natural to assume that at this

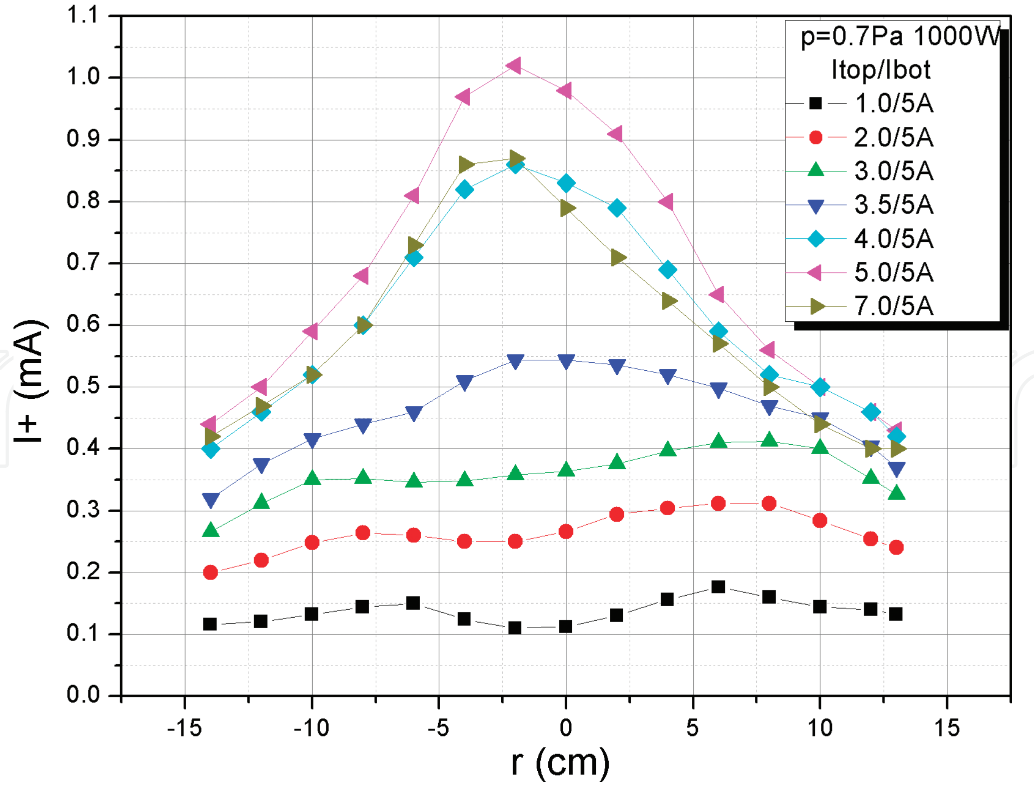

Figure 8.
Radial dependence of ionic saturation current at different top magnet currents while the bottom magnet current is fixed.

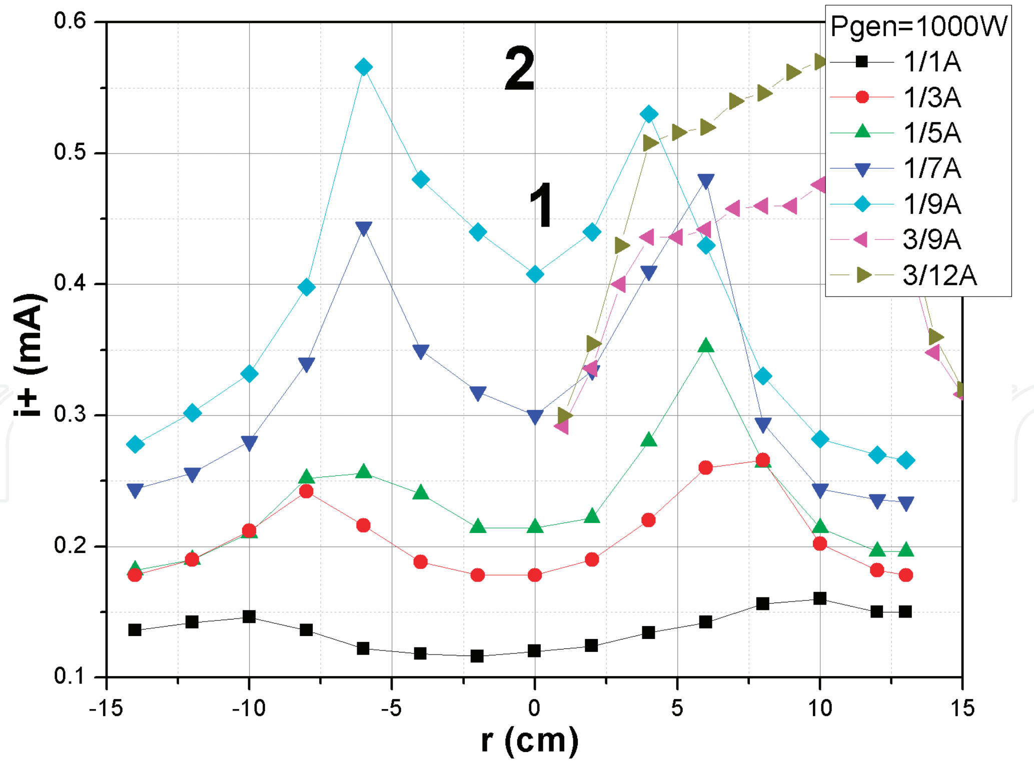

Figure 9.
Radial dependence of the ionic saturation current at different bottom magnet currents while the top magnet current is fixed.

point the RF fields do not yet penetrate the main volume of the plasma. Taking into account that the movement of electrons across the magnetic field is difficult, the distribution of the ionic current with a dip on the axis is observed.

Let us further examine the results of the probe studies in more detail. A typical probe characteristic is shown in **Figure 10**.

As can be seen, the electron energy distribution is close to Maxwell one. **Figure 11** shows the dependence of electron density in the substrate region on the values of currents through the top and bottom magnets at fixed values of current on the top and bottom magnets, respectively.

As can be seen, the range of changes in plasma density corresponds to that which is necessary for the successful implementation of ion assistance technology as part of the magnetron sputtering.

Additional experiments have shown that the best argon pressure range in terms of technological applications is the range between 0.5 and 0.7 Pa. At lower pressures, it is not possible to obtain the required uniformity of the ion current, while an increase in pressure to 1.5 Pa leads to a drop in the values of the ion current.

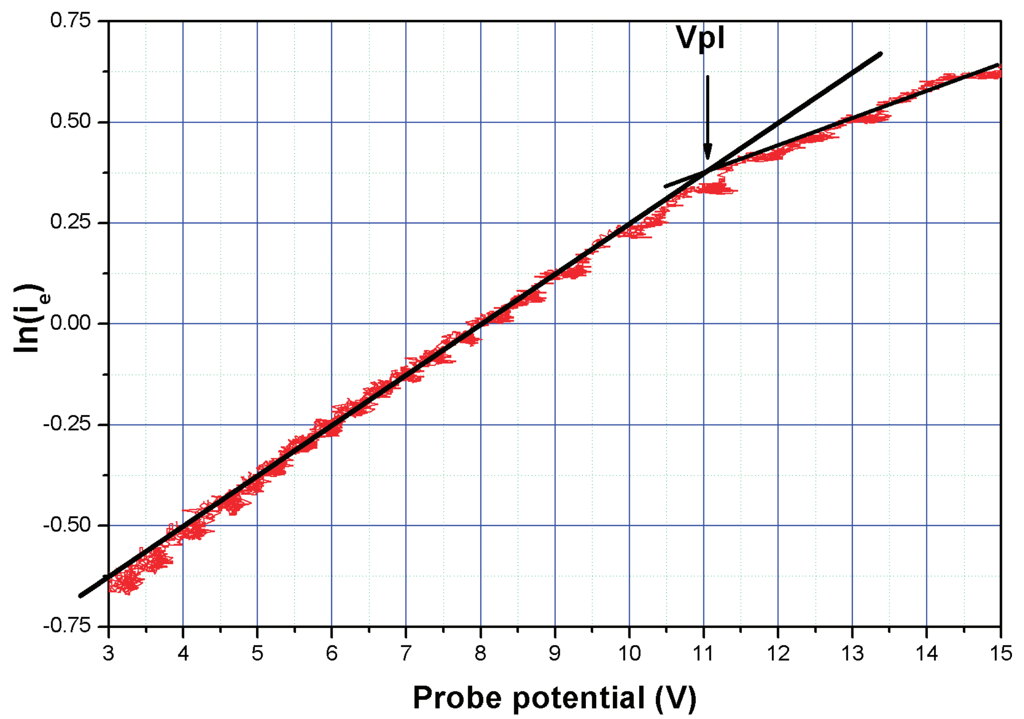

Figure 10.
Dependence of the probe electron current on the probe potential.

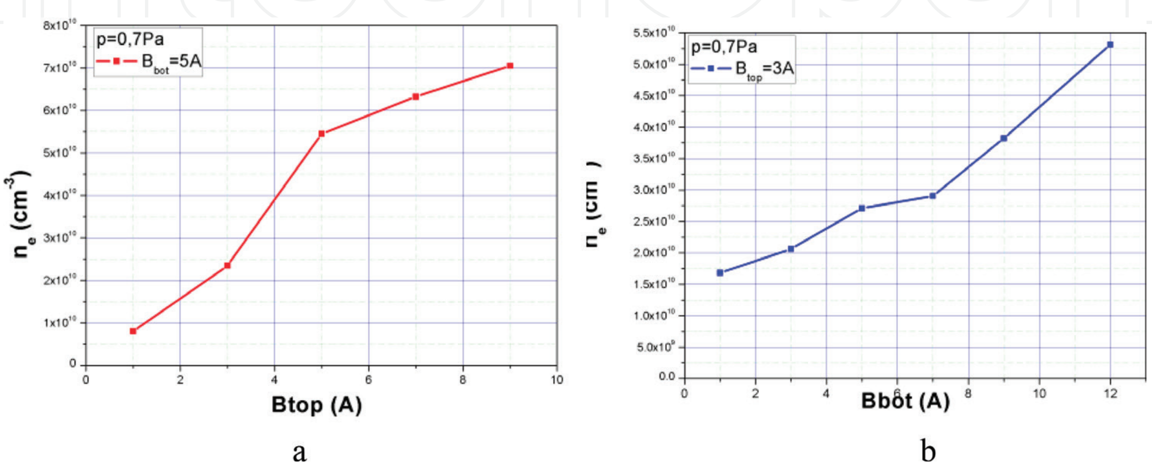

Figure 11.
Dependence of electron density in the substrate region on the values of currents through the top (a) and bottom (b) magnets at fixed values of current on the top and bottom magnets, respectively.

5. Results of the plasma parameter examination when magnetron and gas-discharge sources operate together

At the next stage of the work, the plasma parameters were studied during the simultaneous operation of both the magnetron discharge and inductive RF discharges with external magnetic field. Experiments have shown that the joint operation of magnetron and inductive RF discharges results in a decrease in the threshold pressure, at which magnetron is capable of operating. Titanium spectral lines appeared in the glow spectrum of the magnetron discharge only and at the argon pressure of 0.7 Pa. When magnetron and RF inductive discharges were operating together, the plasma glow spectrum was enriched with titanium lines already at the pressure of 0.3 Pa.

Figure 12 shows the current-voltage characteristics of the magnetron operating at DC mode both independently and together with the gas-discharge source. As can be seen, the sputtering apparatus is capable of operating at substantially lower voltages applied to the cathode.

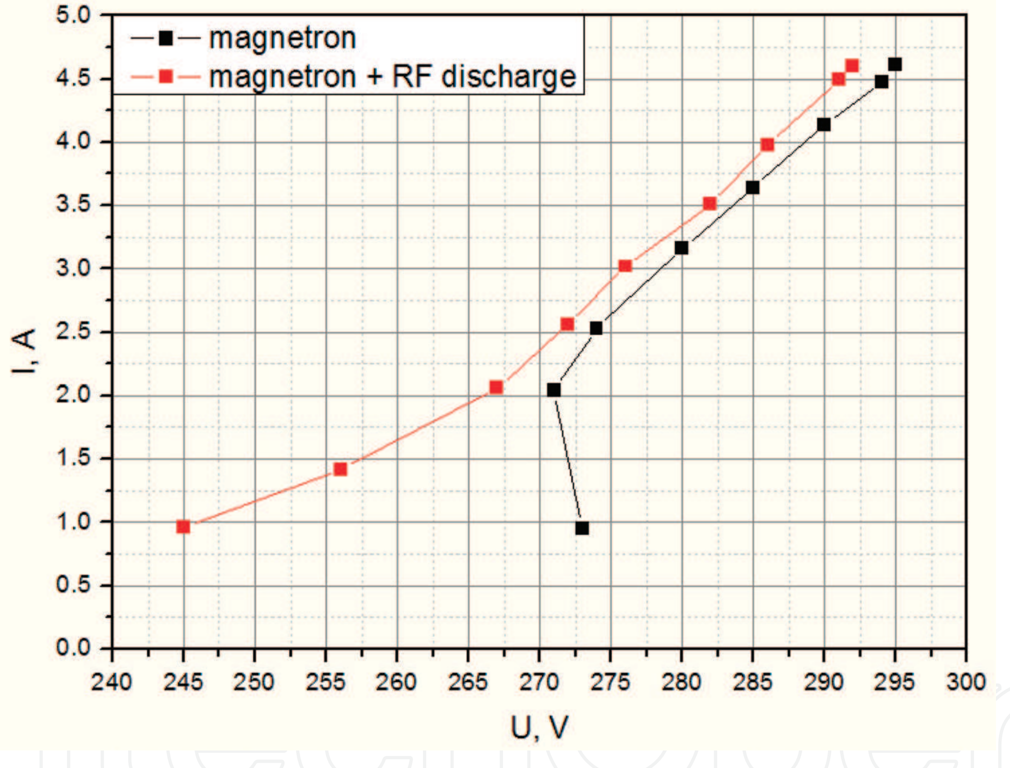

Figure 12.
Current-voltage characteristics of the magnetron operating independently (black curve) and together with the inductive RF discharge with magnetic field (red curve).

6. The effect of assisting ion flow on functional coating structure

To test the effect of ionic stimulation on the properties of functional coatings, thin films were deposited using the magnetron only and using the magnetron and RF sources together with and without applying an additional bias to the substrate. Coatings made of the following materials were used as test samples: Ti, Al, SiAl, SiO_2, and C.

The experiments involving deposition of titanium coatings were aimed at the studying of the effects of the assisting ionic flux magnitude on electro-physical properties of films and their microhardness. It was shown that increase in the power of RF power supply connected to antenna in the range from 0 to 500 W results in almost twofold increase in specific resistivity of the films; at the same time, the microhardness of the films increases by 25%. The observed changes are obviously the result of a change in the film structure. Titanium film morphology studies have shown that the irradiation of films with a flux of accelerated ions leads to a slight decrease in the grain size in the structure of the films. Application of a DC bias to the substrate was accompanied by the smoothing of the surface of films.

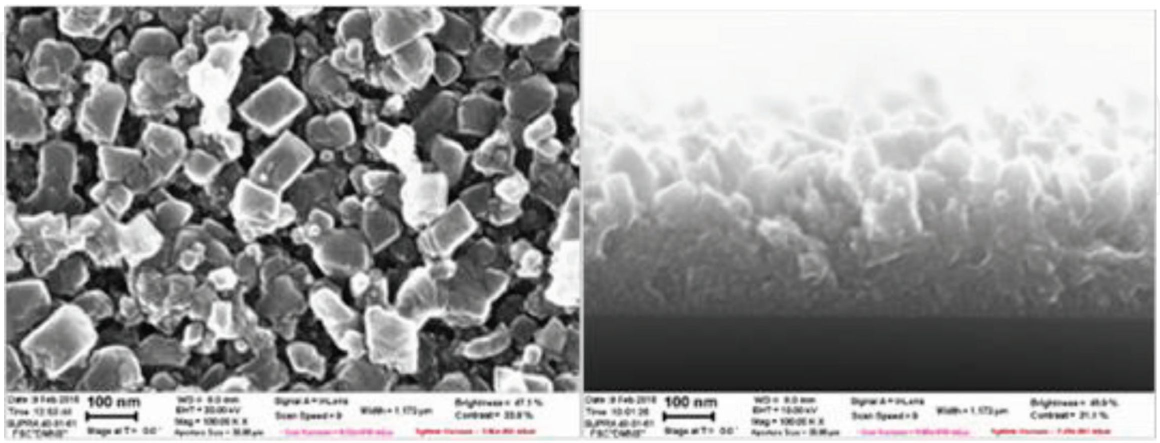

a b

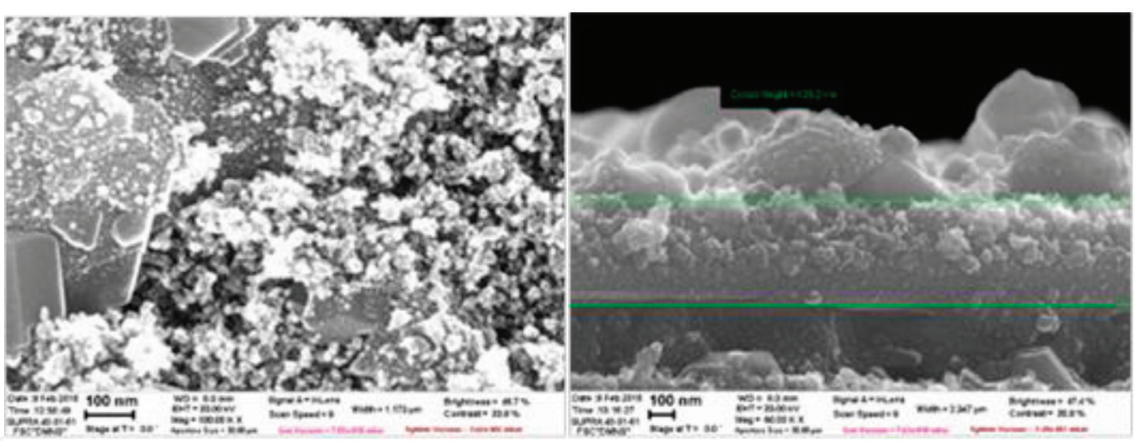

c d

Figure 13.
Aluminum film surface (a and c) and cross-section (b and d).

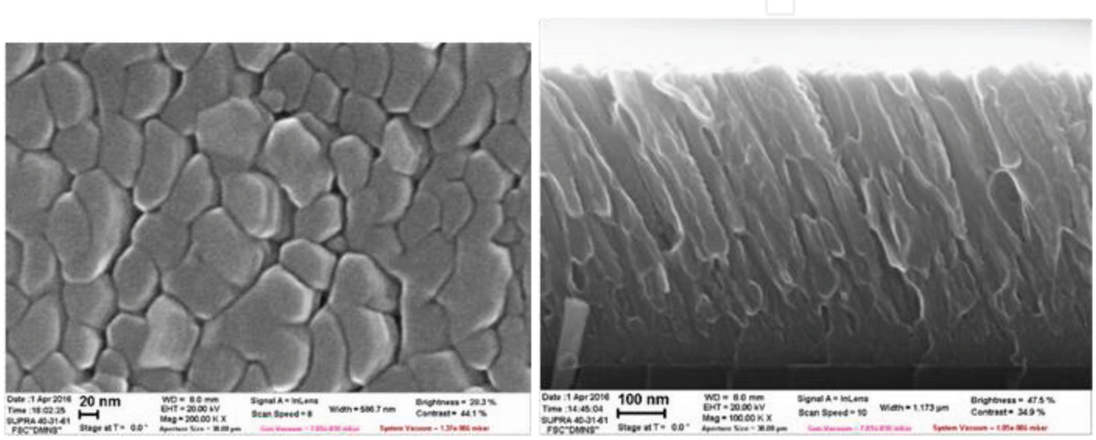

Figure 14.
Film surface and cross-section: Si (Al 10%) deposition, without ionic assistance.

The reduction of grain size in the structure of films in the presence of stimulating ion flux is most clearly seen in the film surface images and the images of aluminum film cleavages, shown in **Figure 13**.

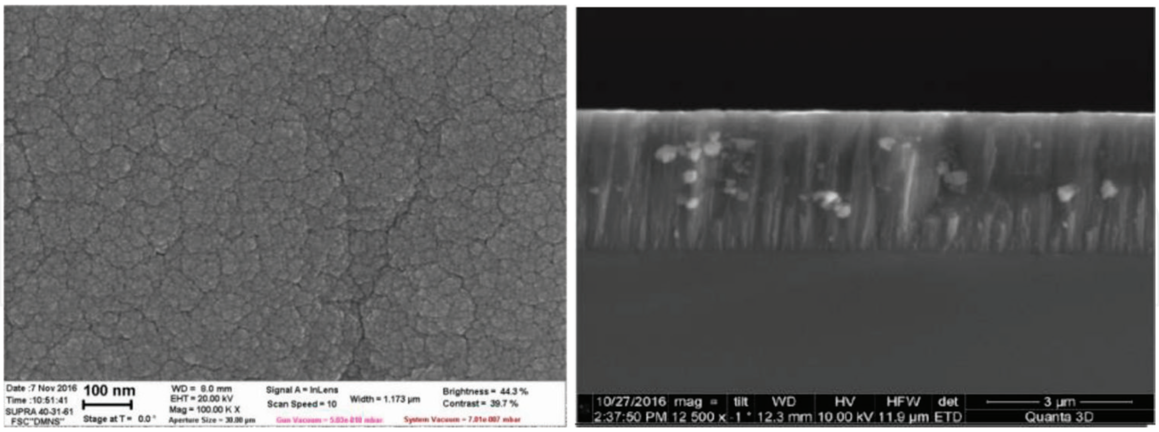

Figure 15.
Film surface and cross-section: Si (Al 10%) magnetron deposition with ionic assistance without applying a bias to substrate.

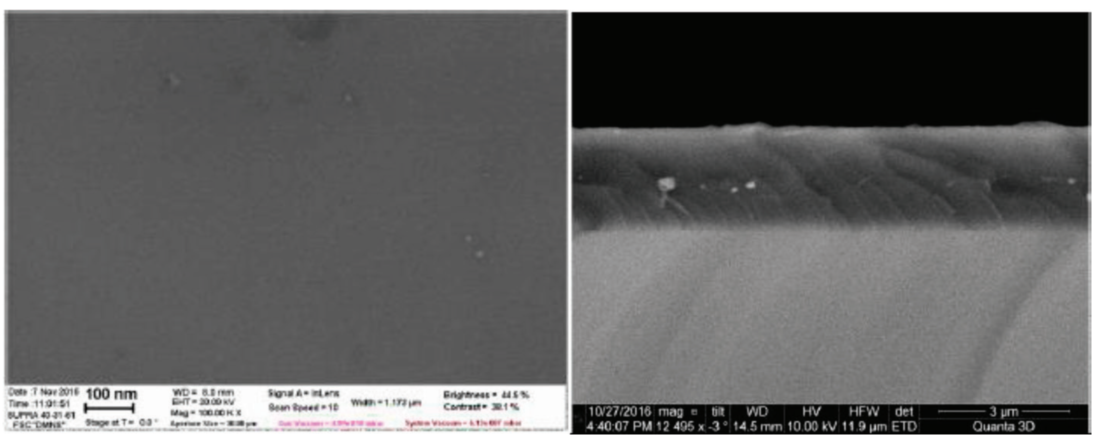

Figure 16.
Film surface and cross-section: Si (Al 10%) magnetron deposition with ionic assistance plus a bias applied to the substrate.

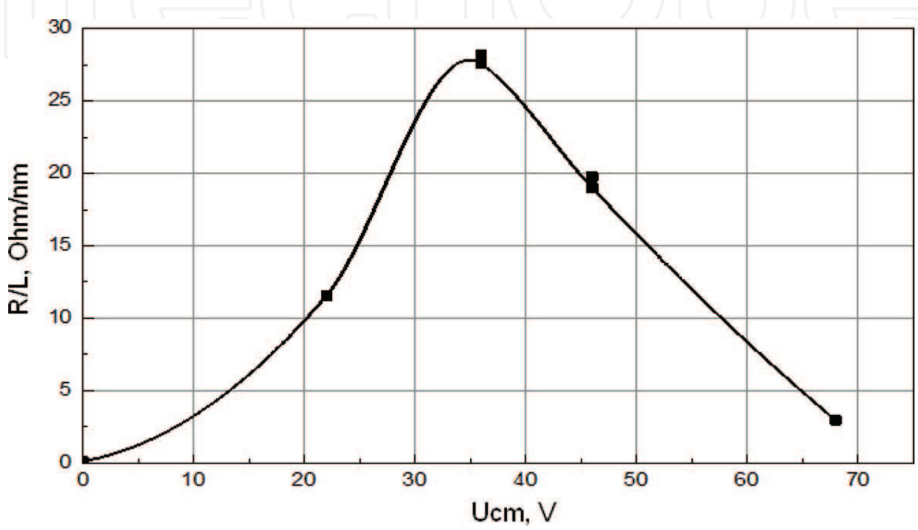

Figure 17.
Dependence of the ratio of film resistance to its thickness on the bias Ucm applied to its substrates.

Interesting results were obtained while depositing silicon with 10% aluminum content. The sample film surface morphology and cleavage are shown in **Figures 14–16**. As can be seen, the samples treated using ionic assistance acquire a columnar structure. When a bias is applied to the substrate, the columnar structure grows at an angle to the normal.

It is known that the ionic stimulation results in significant change in the electrophysical properties of carbon films [28]. **Figure 17** shows the dependence of resistance of a various series of carbon films on the bias voltage [29]. As can be seen, there is a sharp increase in the resistance of the films at the assisting ion energy of 45 eV.

7. Conclusions

The results of the study of plasma parameters in a plasma reactor based on a combination of magnetron and magnetically activated RF discharge indicate the promising outlook as regards to industrial application of the innovative facility. Approaching the region of resonant absorption of RF power by optimizing the magnitude and configuration of the external magnetic field makes it possible to obtain a uniform within 10% radial distribution of the ion current across the diameter of 150 mm. When the RF power supply power is 1000 W, the ion current density on the substrate can be adjusted in the range of 0.1–3 mA/cm^2. The use of ion assisting results in a fundamental change in the structure and properties of functional coatings, deposited using a magnetron.

Acknowledgements

The work was carried out under partial financial support of the RFBR grant 16-02-00646.

Author details

Elena Kralkina[1*], Andrey Alexandrov[1], Polina Nekludova[1], Aleksandr Nikonov[1], Vladimir Pavlov[1], Konstantin Vavilin[1], Vadim Odinokov[2] and Vadim Sologub[2]

1 Physical Faculty of MSU, Moscow, Russian Federation

2 Research Institute of Precision Machine Manufacturing, Zelenograd, Russian Federation

*Address all correspondence to: ekralkina@mail.ru

References

[1] Berghaus B. Improvements in and Relating to the Coating of Articles by Means of Thermally Vaporized Material, U.K. Patent No 510993; 1938

[2] Mattox DM, McDonald JE. Interface formation during thin film deposition. Journal of Applied Physics. 1963;**34**:2493-2494

[3] Mattox DM, Kominiak GJ. Structure modification by ion bombardment during deposition. Journal of Vacuum Science and Technology. 1972;**9**:528-532

[4] Colligon JS. Ion-assisted sputter deposition. Philosophical Transactions of the Royal Society A. 2004;**362**:103-116

[5] Mattox D. The Foundation of Vacuum Coating Technology. N.Y.: Noyes Publications; 2003.534 p

[6] Zhurin VV. Industrial Ion Sources. Broad Beam Gridless Ion Source Technology. N.Y.: Wiley-VCH Verlag & Co; 2012. 382 p

[7] Harper JME, Cuomo JJ, Kaufman HR. Technology and applications of broad beam ion sources used in sputtering. Part II. Applications. Journal of Vacuum Science and Technology. 1982;**21**:737-756

[8] Kaufman HR, Harper JME. Ion assists applications of broad beam ion sources. Proceedings of SPIE. 2004;**5527**:50-68

[9] Petrov IN, Adibi F, Greene JE, Hultman L, Sundgren JE. Average energy deposited per atom: A universal parameter for describing ion-assisted film growth. Applied Physics Letters. 1993;**63**:36-38

[10] Winters H et al. Influence of energy reflected from the target on thin film characteristics. Journal of Vacuum Science and Technology. 1998;**11**:657-663

[11] Rossnagel S. Thin film deposition with physical vapor deposition and related technologies. Journal of Vacuum Science and Technology. 2003;**21**:74-87

[12] Fulton M. Application of ion assisted deposition using gridless end-Hall ion source for volume manufacturing of thin film optical filters. In: Proceedings of Optical Interference Coatings; 1994. p. 2253

[13] Kaufman HR, Robinson RS. Operation of Broad-Beam Sources. Alexandria, Virginia: Commonwealth Scientific Corporation; 1987. 453 p

[14] Shpak A, Rudenko E, Korotash I, Senyuk V, Shamrai K, Odinokov V, et al. Plasma source of low temperature formation of the nanoclusters of metal–catalyst. Nanoindustry (Russian Federation). 2009;**4**:12-15

[15] Aleksandrov AF, Vavilin KV, Kral'kina EA, Neklyudova PA, Nikonov AM, Pavlov VB, et al. Plasma parameters in the reactor with simultaneous magnetron discharge and inductive radio-frequency discharge in the presence of external magnetic field. Journal of Communications Technology and Electronics. 2018;**63**:374-380. DOI: 10.22184/1993-8578.2016.70.8.104.108

[16] Aleksandrov AF, Petrov AK, Vavilin KV, Kral'kina EA, Neklyudova PA, Nikonov AM, et al. Influence of external conditions on physical processes and plasma parameters in a model of a high-frequency hybrid plasma system. Russian MicroElectronics. 2016;**45**:433-441

[17] Aleksandrov AF, Petrov AK, Vavilin KV, Kralkina EA, Neklyudova PA, Nikonov AM, et al. Investigation of the helicon discharge plasma parameters

in a hybrid RF plasma system. Plasma Physics Reports. 2016;**42**:290-292. DOI: 10.1132/S1063780X16030016

[18] Vavilin KV, Kralkina EA, Nekludova PA, Petrov AK, Nikonov AM, Pavlov VB, et al. Hybrid plasma system for magnetron deposition of coatings with ion assistance. Journal of Physics Conference Series. 2015;**669**:1-4. DOI: 10.1088/1742-6596/669/1/012033

[19] Johnson WL. Electrostatically-shielded inductively-coupled RF plasma source. In: Popov OA, editor. High Density Plasma Sources. NY: Noyes Publications; 1996. pp. 100-114

[20] Chen FF. Helicon plasma sources. In: Popov OA, editor. High Density Plasma Sources; 1996. pp. 1-75

[21] Shinohara S. Helicon high density plasma sources: Physics and applications. Advances in Physics. 2018;**3**(1):1420424. DOI: 10.1080/23746149.2017.1420424

[22] Chen F. The low-field density peak in helicon discharges. Physics of Plasmas. 2003;**10**:2586-2592. DOI: 10.1063/1.1575755

[23] Chen FF, Jiang X, Evans JD, Tynan G, Arnush D. Low-field helicon discharges. Plasma Physics and Controlled Fusion. 1997;**39**:A411-A420

[24] Kral'kina EA. Low-pressure radio-frequency inductive discharge and possibilities of optimizing inductive plasma sources. Physics-Uspekhi. 2008;**51**:493-512. DOI: 10.1070/PU2008v051n05ABEH006422

[25] Kralkina EA, Rukhadze AA, Nekliudova PA, Pavlov VB, Petrov AK, Vavilin KV. RF power absorption by plasma of low pressure low power inductive discharge located in the external magnetic field. AIP Advances. 2018;**8**:035217. DOI: 10.1063/1.5023631

[26] Chen FF, Jiang X, Evans JD. Plasma injection with helicon sources. Journal of Vacuum Science and Technology A. 2000;**18**:2108-2115. DOI: 10.1116/1.1289537

[27] Petrov AK. Physical processes in the two-chamber inductive RF plasma source with the external magnetic field [thesis]. Moscow: Physical faculty of Moscow State University; 2016 [in Russian]

[28] Guseva MB, Savchenko NF, Babaev VG. The influence of ion irradiation on the structure and properties of amorphous carbon films. Radiation Effects Letters. 1986;**87**:215224

[29] Grushin M, Kralkina E, Nekludova P, Nikonov A. Influence of the ion assistance on the physical properties of the carbon films obtained by the magnetron sputtering. In: Proceedings of the Conference "Low Temperature Plasma in the Processes of Functional Coatings Deposition". Kazan; 2018 [in Russian]